Construction of Phase-I Insertion Devices at TPS

Taiwan Photon Source (TPS), a third-generation light source based on a 3-GeV storage ring, is featured with high brilliant insertion devices (ID). Synchrotron radiation (SR) generated from undulators can cover both soft and hard X-ray energy spectra. The scope of TPS Phase-I ID includes seven in-vacuum undulators for X-ray photon sources and three elliptically polarized undulators (EPU) for soft X-ray photon sources. Construction of Phase-I ID was completed in 2014. This report describes the required field qualities and important techniques implemented in the TPS insertion devices.

Introduction

To generate high brilliant light from a third-generation light source is the key motive and drive to develop an insertion device. Of two typical approaches for generating high brilliance photons, one is to improve the quality of the electron beam. Constructing a storage ring of low emittance, such as at TPS, NSLSII, and MAX IV, becomes important to pursue a diffraction-limited light source. Another approach is to improve the quality of the photon beam of the light source. In general, the quality of the photon beam is associated with angular divergence, monochromaticity and the photon flux density. A light source generated from an undulator typically has all three excellent characteristics. The angular divergence of undulator radiation is proportional to $1/\sqrt{N}$ where N denotes the number of undulator periods. The photon flux density is proportional to N^2, whereas the radiation bandwidth associated with monochromaticity is proportional to N^{-1}. According to these criteria, many undulator periods are preferable. However, the operation of a long undulator with many periods in a straight section is bounded by the vertical betatron function. As the vertical betatron function increases quadratically along the longitudinal direction and suffers interference from a small magnet gap at the end of the undulator, a large beam loss and short beam lifetime might occur in a small undulator gap. To maximize the life time of the beam, the maximum length of an undulator, which depends on the vertical betatron function, must be less than twice the vertical betatron function.

Undulators in Taiwan Photon Source

The plan for TPS Phase-I ID includes seven sets of in-vacuum undulators and EPU in three sets. The beamlines of TPS phase-I experimental facilities and type of insertion devices are shown in Table 1. In a long straight

Table 1: Beamlines and light sources for TPS phase-I experimental facilities.

Beamlines	Light source	Max K_y/K_x	Energy range
Protein Microcrystallography	IU22-3m	1.47	5.7 - 20 keV
Resonant Soft X-ray Scattering	EPU48x2	3.72/2.47	0.40 - 1.50 keV
Submicron Soft X-ray Spectroscopy	EPU46	3.48/2.32	0.35 - 1.50 keV
Coherent X-ray Scattering	IU22-3m+IU22-2m	1.47	5 - 20 keV
Submicron X-ray Diffraction	IUT22-3m	1.47	7 - 25 keV
X-ray Nanoprobe	IU22-3m	1.47	4 - 15 keV
Temporally Coherent X-ray Diffraction	IU22-3m+IU22-2m	1.47	5.6 - 25 keV

section, special beam optics with quadrupole-triplet is designed to contain two subsections with a mini-vertical beta function. Double segmented undulators with a small gap can thus be installed in a long straight section without sacrificing the beam lifetime. Double EPU48 and double in-vacuum undulators (IU22-3m and IU22-2m) are placed inline to enhance the photon source if two undulators radiate coherently. Submicron X-ray diffraction requires pink light source with bandwidth of energy spectrum up to 10%, so that in-vacuum undulator with tapered function is required.

Undulator Field Quality

To ensure a high brilliant light source and stable operation of the storage ring, stringent field quality of an undulator is demanded. The root mean square (RMS) phase error is a parameter commonly used to assess an undulator quality. Phase error describes phase distribution of emissions from each undulator pole and all emissions shall be in phase to avoid reduction of brilliance. In the case of TPS, high harmonics radiation from undulator shall be used for the X-ray source and consequently the RMS phase error shall be less than 3 degrees. The maximum spectral intensity of the first to ninth harmonic undulator spectra is decreased less than 20% from the ideal case of an undulator. First-integral deviations and kicker value of half undualtor period are associated with deviation of maximum magnetic field and undulator period length. If the first-integral deviations and kicker value are small, the electrons travel in a straighter trajectory.

A special design of end pole is important to ensure that the offset and steering of the electron beam are zero and independent from the setting of an undulator gap. Table 2 shows the specifications of the TPS undulator performance and all undulators satisfy these requirements.

In-Vacuum Undulator

Using a mini-gap in-vacuum undulator with a short period to obtain X-rays of short wavelength is an optimal usage. An in-vacuum undulator is designed to have magnets array inside a large vacuum chamber and allow the entire magnet gap to be fully used by a physical aperture. The magnet of a TPS in-vacuum undulator has a conventional hybrid structure with NdFeB magnets. The coercivity enhancement in the magnet is adapted to dysprosium diffusion technology and the radiation resistance of magnet is improved. As a result, a sufficient magnetic field is achievable with a small period length. The vacuum system of an IU22-2m device consists of four NEG pumps (SAES MK500-SP8, 500L/s) and two Ion pumps (Canon Anelva PIC-052NP 125L/s) to ensure a sufficient pumping capacity.

Table 2: TPS undulator specifications.

		In-vacuum undulator	Elliptically polarized undulator	Comment
RMS deviation of d*I*/*I*		<0.5%		At all gaps
Trajectory straightness		< ±2 μm < ±3 mrad		*K*>1
Multipole components	Dipole Quadrupole Sextupole Octupole	<100 G cm <50 G <100 G/cm <100 G/cm^2		*K*>1
Phase errors		<3°	<3° (linear) <5°(circular)	*K*>1
Maximum field		>1.01 T	>0.83 T (horizontal linear) >0.55 T (vertical linear)	At minimum gap

**K* denotes the undulator deflection parameter.

Thermal Challenge

The beam-induced heat load on an in-vacuum undulator with a small gap is a critical issue because TPS is designed to operate in high current and short bunch length. Protective solutions to avoid a large power density on a magnet foil are carefully implemented, such as a vertical photon absorber and satisfactory flat magnet foil. A magnet foil is made of nickel-plated copper, Cu-Ni, sheet. As copper foil has adequate thermal conductivity and a nickel layer provides a satisfactory contact through a magnetic attractive force, all in-vacuum undulators use a Cu-Ni foil to create a smooth surface on top of the magnet to reduce the wake-field and image-current induced by bunched beam.

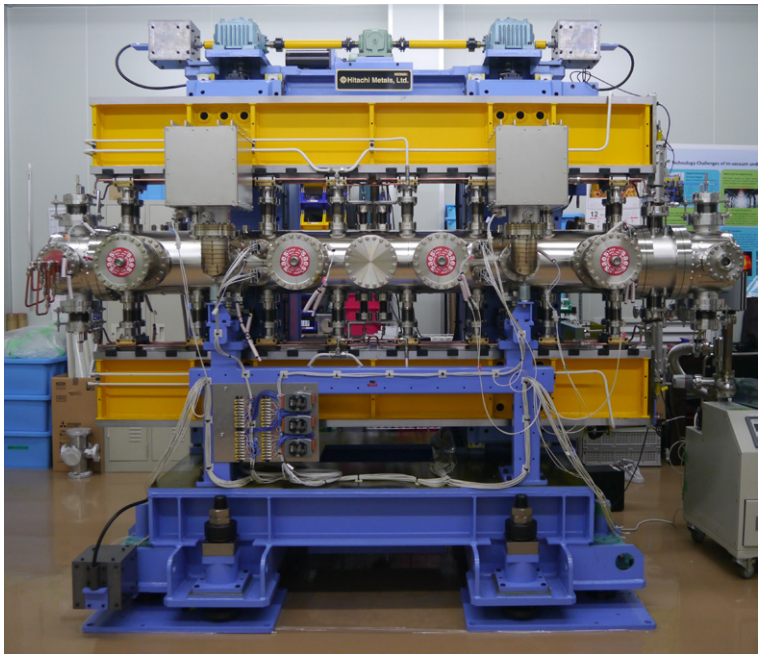

Fig. 1: In-vacuum undulator with period length of 22 mm, magnet length 2.124 m.

A TPS in-vacuum undulator will experience large heating from the image current that derives from the short bunch-length and a large beam current. Such power density per unit length, 15.7 W/m, exceeds the empirical safety limit, 10 W/m.[1] An efficient way to avoid such kind of heat load of image-current in a small-gap on in-vacuum undulator is thus to have long bunch length operation. The designed bunch length, 9.5 ps, is for low bunch current. Bunch lengthening effects is a function of the beam current. Lengthening of the bunch is expected, if the number of filling bunches is reduced in operation or a harmonic cavity installed.

The flatness of the foil is important to ensure that undulator gaps will not decrease further and affect the clearness for synchrotron light and electrons. Small bumps on a foil might occur after baking and might result in a catastrophic avalanche meltdown of the foil. SR striking the bumps generates more heating power than that from image-current heating. SR is the main heat source for an avalanche meltdown. Image-current heating is an indirect source, but a large image current decreases the threshold of an avalanche meltdown. Magnet foils of a TPS in-vacuum undulator use nickel (thickness 50 μm) to improve the contact force between the foil and the magnet. The risk of foil deformation might be diminished.

Vertical Photon Absorber

In the TPS double-undulator system, if two synchronized undulators operate at a minimum gap of 5 mm, the first in-vacuum undulator, ID1, receives radiation from the bending magnet and the upstream part of the undulator. The maximum linear power density is 2.83 W/m at the end of the magnet array. At the second undulator, ID2, the irradiated power on a magnet surface comes from upstream bending magnet, undulator and itself. As the radiating angle varies with the irradiated position, the maximum total power density of SR at the end of a magnet array can attain 68.0 W/m.[1] High risk of an avalanche meltdown might materialize to the magnet foil. The technical action taken for the TPS double-undulator

system is to install vertical photon absorbers in of front the ID2 magnet array to cut off most radiation from upstream bending magnet and undulator. Figure 1 also shows a vertical photon absorber assembled at the upstream of an undulator. The vertical photon absorber not only blocks SR from an upstream undulator but also protects magnets from mis-steered electron beams.

UHV Bakeout

Baking an in-vacuum undulator that artificially accelerates outgassing is a most important and challenging process in construction of an in-vacuum undulator. The magnet of the type used in IU22 has great coercivity, 2760 kA/m, and was annealed at 145 °C before being assembled into the undulator. The magnets can thus endure a temperature up to at least 125 °C without demagnetization. Control of temperature is important to avoid demagnetization and deformation of vacuum components of the undulator or deterioration of mechanical properties. After baking for 72 hours, the final pressure can achieve less than $3x10^{-8}$ Pascal. The spectrum of the residual gas provides information to identify the nature of the residual gases from an in-vacuum undulator, shown in Fig. 2.

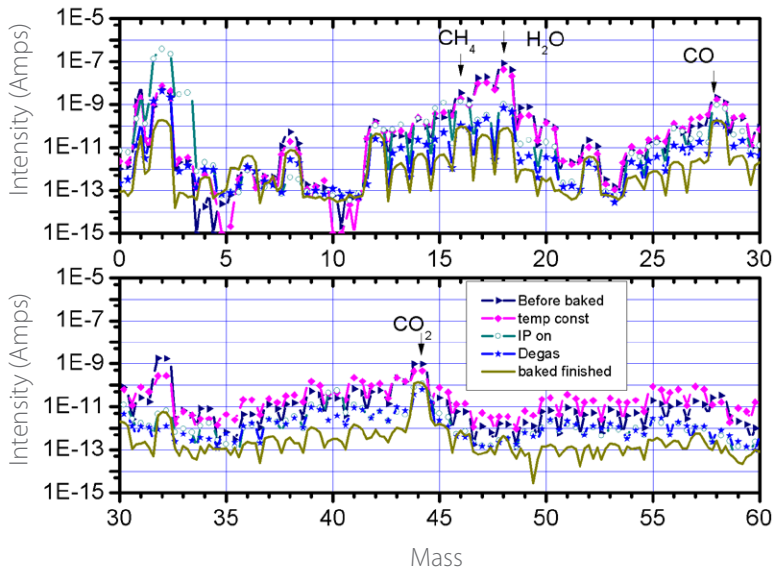

Fig. 2: Residual gas spectra of an undulator system in vacuum during baking. (Reproduced from Ref. 2)

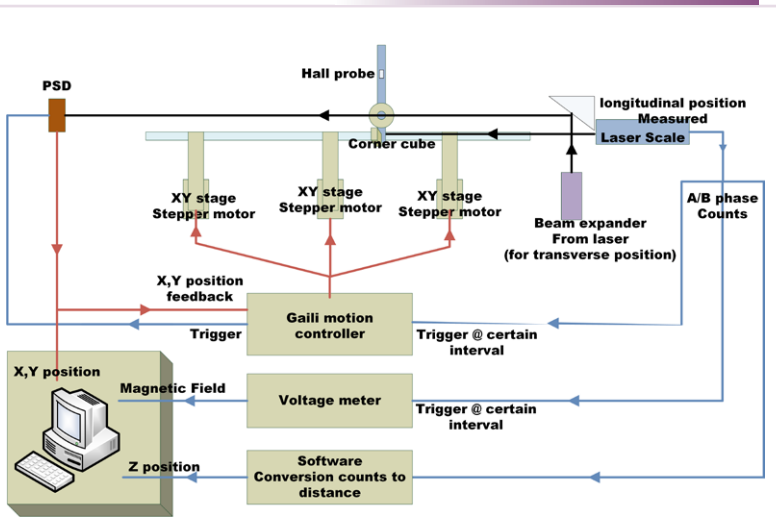

Fig. 3: Control diagram for an in-situ measurement system.

Laser-Aligned Hall-Probe Measurement System

One challenge in development of an undulator is to measure the magnetic field to ensure that it does not vary during assembly of the vacuum components and after transport over a large distance. A laser-aligned Hall-probe measurement system was designed in a very compact form and with great accuracy to fit inside the vacuum chamber. The position of the Hall probe was aligned with a laser system.[3] The horizontal and vertical positions of the Hall probe were detected by a phase sensitive detector and when the Hall probe was detected in a position off the magnetic axis, three XY stages simultaneously adjusted the Hall probe back to a position on the axis (Fig. 3). Feedback algorithms were implemented to ensure that the center of the Hall probe coincided with the center of the magnetic field during the measurements. Laser-

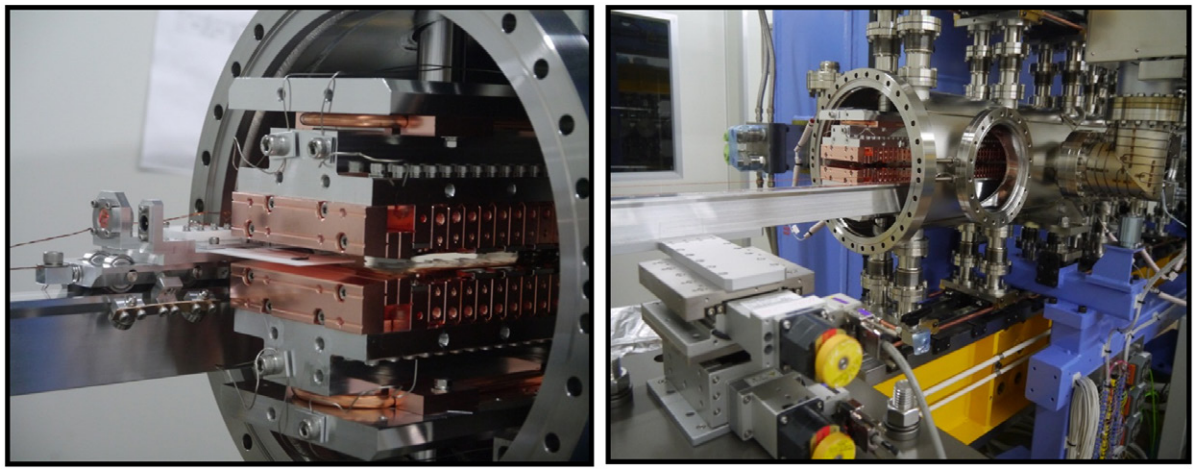

Fig. 4: In-situ measurement system.

aligned Hall-probe measurement system is shown in Fig. 4. which is designed and built by magnet group. The repeatability of the Hall probe position is 5.6 μm and the RMS phase error is 0.1°. The calibration measurement of field deviation from in-situ system shows only a small difference relative to the traditional measurement system on a granite bench. The measurement system can be developed further for use in an evacuated or cryogenic environment.

Elliptically Polarized Undulator

The most widely used helical undulator is APPLE-II type elliptically polarized undulator for varied polarization with a high degree of polarization. The upper and lower magnet arrays are split in half at the transverse center. When the diagonally opposed magnet arrays are moved axially, the polarization alters. There is an air gap between the magnets and the transverse uniformity is small relative to a planar undulator. Transverse field uniformity might generate a large dynamic integral and nonlinear field seen along the trajectory of the electron. In a worst-case scenario, a nonlinear field causes a tune shift and poor injection efficiency. Dynamic and static integrals vary with the polarization phase mode, and as a result the performance of an EPU might degrade in some polarization phases. In TPS EPU, the size and location of iron shim pads are carefully calculated to be placed on top of the magnet, which decreases the phase-dependent issue on both static and dynamic integrals.

Mechanical Frame

Moving magnet arrays generates strong magnetic forces between adjacent arrays, so that a strong mechanical frame is critical to ensure a stable quality of magnetic field during a polarization switch. The design, manufacture and assembly were completed in the NSRRC (Fig. 5). The maximum variation of an undulator gap along the longitudinal direction is 20 μm at the maximum magnetic force loading of 35 kN. This gap variation creates an initial phase error of 3.4 degrees. Magnet shimming is hence performed to compensate the gap-induced errors. Subsequently, the repeatability of the gap in various polarization modes is reduced to less than 2.5 μm, which ensures that a deviation of the photon energy is less than one tenth of the intrinsic width at the fifth undulator harmonic.

Optimization of Performance of the Magnetic Field

Despite the highly accurate and robust mechanical frame, the quality of the magnetic field yet needs to be controlled through sorting and shimming. This field correction scheme is developed in the NSRRC and successfully implemented in EPU48 construction. In magnet sorting strategies, the first step is to sort individual blocks measured with a Helmholtz coil. RADIA code assists to arrange magnet blocks into sub-modules based on results of minimum phase error in various polarization modes. The second step is to sort the magnet sub-

modules based on a simulated-annealing algorithm to eliminate an influence from the inhomogeneity and imperfections of the blocks. Since some local-field errors remain, a two-step shimming algorithm is used to eliminate phase error and static multipole error. The first step is to improve the phase error and thereby the straightness of a trajectory. The second step is to decrease the residual-field integral using a magic finger that uses an arrangement of small magnetic chips at the extremities of the EPU. The best arrangement of chips is also calculated with a simulated-annealing algorithm.

Figure 6 shows the results of the straightness of the horizontal and vertical trajectories in all phase modes. After the two-stage sorting, the straightness has been improved within ±11 μm. After shimming, it has been further improved within ±4 μm in all operating modes. (Reported by Jui-Che Huang)

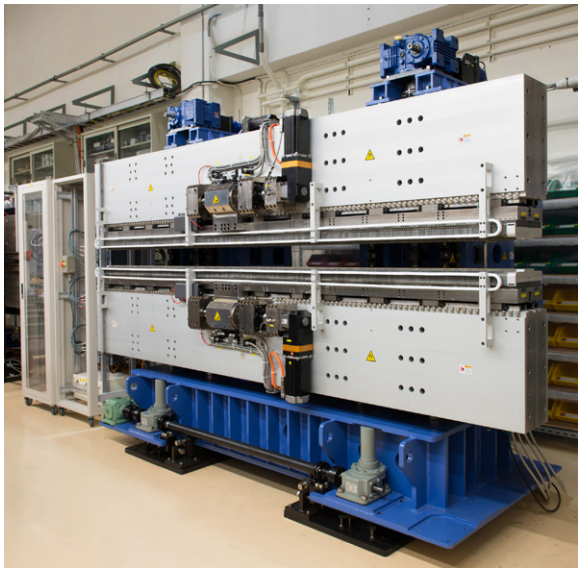

Fig. 5: EPU48 constructed in the NSRRC.

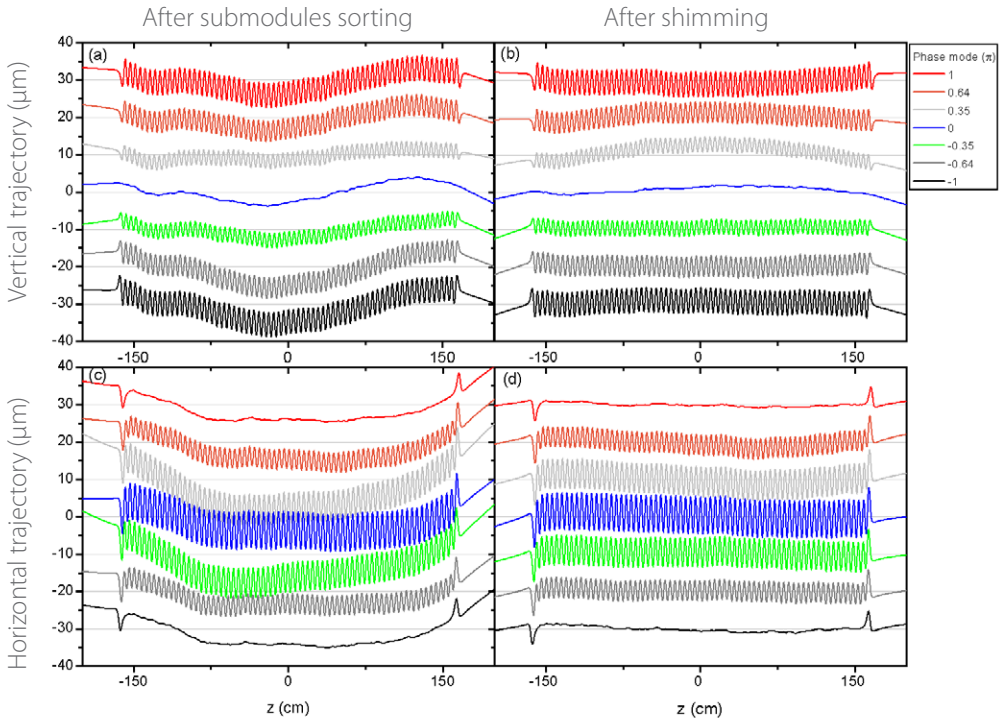

Fig. 6: Straightness of (a,b) vertical and (c,d) horizontal trajectories; (a,c) before shimming, (b,d) after shimming. (Reproduced from Ref. 4)

References

1. J.-C. Huang, H. Kitamura, C.-H. Chang, C.-H. Chang, and C.-S. Hwang, Nucl. Instr. Meth. Phys. Res. **775**, 162 (2015).
2. J.-C. Huang, L.-H. Wu, C.-K. Yang, C.-K. Chuan, T.-Y. Chung, and C.-S. Hwang, IEEE J. Supercondu., **24**, 4100705 (2014).
3. C.-K. Yang, C.-H. Chang, C.-S. Hwang, J.-C. Huang, and T.-Y. Chung, IEEE J. Supercondu. **24**, 1649604 (2014).
4. T.-Y. Chung, C.-H. Chang, C.-Y. Wu, J.-C. Huang, F.-Y. Lin, J.-C. Jan, C.-H. Chang, and C.-S. Hwang, IPAC. TUOCB03 (2014).